Design and Development of Miniature Parallel Robot for Eye Surgery

Tomoya Sakai, Kanako Harada, *IEEE Member*, Shinichi Tanaka, *IEEE Student Member*, Takashi Ueta, Yasuo Noda, Naohiko Sugita, and Mamoru Mitsuishi, *IEEE Member*

***Abstract*— A five degree-of-freedom (DOF) miniature parallel robot has been developed to precisely and safely remove the thin internal limiting membrane in the eye ground during vitreoretinal surgery. A simulator has been developed to determine the design parameters of this robot. The developed robot's size is 85 mm × 100 mm × 240 mm, and its weight is 770 g. This robot incorporates an emergency instrument retraction function to quickly remove the instrument from the eye in case of sudden intraoperative complications such as bleeding. Experiments were conducted to evaluate the robot's performance in the master-slave configuration, and the results demonstrated that it had a tracing accuracy of 40.0 μm.**

I. Introduction

In ophthalmology, vitreoretinal surgery [1] is one of the most difficult microsurgical operations to perform. In this surgery, 2–3 microsurgical instruments (size: ~0.7 mm) are inserted through cannulas placed in the sclera, and the surgeon manipulates them using stereo-microscopic vision. Surgical tasks include peeling of the internal limiting membrane (ILM, thickness: ~3μm) and drug injection into blood vessels (diameter: ~60 μm) using a micropipette. Vitreoretinal surgery is minimally invasive and therefore beneficial for patients; however, it requires considerable skill to perform. The surgeon needs to manipulate small, fragile tissues using thin, long instruments in a small space with high accuracy. The surgeon needs to suppress hand tremors, whose amplitude is ~100 μm [1], when handling such tissues. The force applied on the retina needs to be well controlled because excessive force can cause permanent tissue damage that could, in the worst case, result in blindness.

In this light, researchers have strongly focused on providing robotic aids for facilitating such difficult surgical tasks. Eye surgical devices and robots including Steady-Hand [2], Micron [3], and Robotic Manipulator for Retinal Surgery [4] have been developed. A master-slave parallel robot system for eye surgery [5] and a master-slave microsurgical robotic system for eye surgery [6] have also been developed. Master-slave control enables a surgeon's hand motion to be replicated using an adjustable motion scaling ratio as well as filtering of hand tremors. Therefore, it is preferable for precise and dexterous manipulation in a small space. From our experience, we think that miniaturizing and reducing the weight of the slave robot in the previously developed master-slave parallel robot system [5] would be promising for clinical applications. This paper describes the requirements and design of a miniature parallel robot for eye surgery. An emergency instrument retraction function was newly implemented to make the surgery safer.

This research was partially supported by the Grant-in-Aid for Scientific Research (S) 23226006 and the Grant-in-Aid for Young Scientists (A) 26700023 from the Japan Society for the Promotion of Science (JSPS).

T. Sakai, K. Harada, S. Tanaka, T. Ueta, Y. Noda, N. Sugita, and M. Mitsuishi are with The University of Tokyo, Bunkyo-ku, Tokyo 113-8656, Japan (phone: +81-3-5841-6357; e-mail: kanako@nml.t.u-tokyo.ac.jp).

II. Miniature Parallel Robot for Eye Surgery

A. Requirements

Fig. 1 shows the required size and dimensions for the newly designed miniature parallel robot for eye surgery based on our previously developed parallel robot [5].

- Workspace: The diameter of the eye is ~24 mm, and that of the target region in the eye ground is ~5.5 mm. Therefore, the robot workspace is determined to be 7 mm in diameter considering individual differences among patients and for easier operation around the edge of the target region.
- Degrees of freedom (DOFs): Surgical instruments used for vitreoretinal surgery include a light probe, a vitreous cutter, a micropipette, and a forceps. The positioning of each instrument requires three DOFs—two for the pivoting motion around the insertion point and one for the translational motion along the tool axis. Additionally, instruments with an asymmetrical tip require 1-DOF rotation around their axis. A forceps requires one additional DOF for gripping.
- Remote center of motion (RCM): A robot for vitreoretinal surgery needs to have an RCM; however, perfect stabilization of the instrument at the RCM point is difficult owing to backlash. Motion errors at the RCM (i.e., instrument insertion) point may cause a large force to be applied at this point, potentially damaging the eye. Therefore, such errors should be sufficiently small. The maximum motion error was limited to 3 mm based on medical doctors' advice.
- Positioning resolution and accuracy: Considering the target size, the positioning resolution was determined to be 15 μm. As for the accuracy, the previously developed robot had an accuracy of approximately 20 μm in the tracing task [5], and thus an equivalent or better accuracy is required. A higher performance of tool positioning could be preferable from a clinical viewpoint, but this requirement was determined from a compromise between the requirement and commercially available actuators.

978-1-4244-7929-0/14/$26.00 ©2014 IEEE

- Emergency instrument retraction: Actuators with high precision generally move slowly; however, they should be quickly retractable in case of emergency (e.g., bleeding). Therefore, the robot must have an emergency instrument retraction mechanism. The retraction distance was determined to be 30 mm to safely retract the instrument from the eye of 24-mm diameter. The activation of this mechanism should be independent of the control system of the robot so that it is feasible even in case of system failure.
- Sterilizability: For clinical use, the instrument should be easily separated from the robot. A separating unit connecting the instrument and the robot can facilitate the same without risking contamination.
- Size and weight: Miniaturization and weight reduction of the surgical robot should facilitate its use in an operation room and eventually reduce its cost. Considering the previously developed parallel robot [5], the new robot should be smaller than 100 mm × 100 mm × 250 mm and lighter than 1000 g.
- Positioning of robot: The robot needs to be placed in a narrow, 190-mm gap between the microscope and the eye without interfering with the microscopic view.

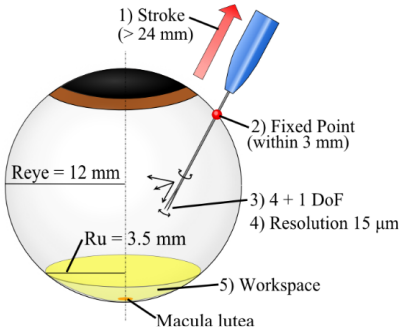

Fig. 1 Requirements for workspace dimensions and degrees of freedom

B. *Parallel mechanism*

Fig. 2 shows the model of the parallel mechanism, called the PUS mechanism [7], comprising links and prismatic, universal, and ball-and-socket joints. The ball-and-socket joints at the end plate can be replaced using bearings enabling rotational motion along each axis. The axes of six prismatic joints are arranged at the same distance from the center of the base plane. The origin *O* of the coordinate system of the robot {M} is at the center of the fixed plane connecting the end points (L_{bi}) of the prismatic joints with zero displacement (i.e., initial state). In the figure, T denotes the instrument tip; C, the connecting point of the instrument to the end plane; F, the RCM point; L_{eff}, the instrument length; L_c, the link length; R_e, the distance from the center of the end plate to each ball-and-socket joint; D_e (<60°), the angle between the paired joints; R_b, the distance from the center of the base to the end of each prismatic joint; D_b (<60°), the angle between the paired prismatic joints; and L_{max}, the maximum translation distance of the prismatic joint. L_{bi} and L_{ei} denote the end points of the *i*-th link. Bold lowercase letters indicate vectors to each defined point.

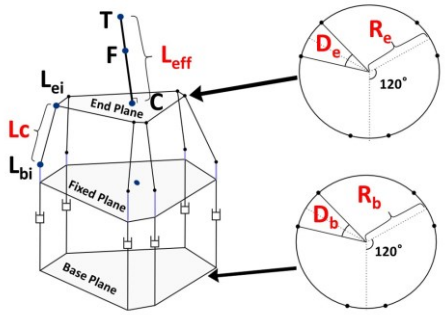

Fig. 2 Model of parallel mechanism

The unit vector in the instrument's direction **n** is given as

$$\mathbf{n} = \frac{\boldsymbol{t} - \boldsymbol{f}}{|\boldsymbol{t} - \boldsymbol{f}|} \tag{1}$$

Fig. 3 shows the angle of the instrument to the microscope θ_0 and the rotation matrix **R** of the coordinate system that represents an extrinsic rotation with Euler angles α, β, and γ about the z, y, and x axes, respectively.

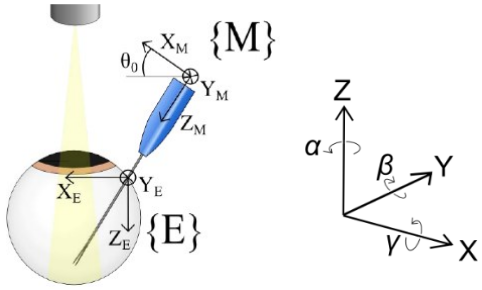

Fig. 3 Coordinate system

The parallel mechanism has a small rotational angle around the instrument axis, and therefore, only 3 DOFs were used by imposing the constraint α = 0; instead, 2-DOF mechanisms for instrument manipulation were implemented on the end plate. Specifically, 2-DOF pivoting motion around the RCM point and 1-DOF translational motion along the instrument axis were realized by the parallel mechanism, and therefore, a rotational actuator for instrument rotation around its axis and a prismatic actuator for the grasping motion of the forceps were mounted on the end plate. Under this constraint, the unit vector **n** is equal to the third column of the standard basis vector of the coordinate system {M} rotated by **R** by the actuation of the prismatic actuators, and therefore, the following equation is obtained:

$$\begin{pmatrix} \alpha \\ \beta \\ \gamma \end{pmatrix} = \begin{pmatrix} 0 \\ \sin^{-1}(n_x) \\ \sin^{-1}\left(-n_y / \sqrt{1 - n_x^2}\right) \end{pmatrix} \tag{2}$$

where n_x and n_y are the x and y elements, respectively, of vector **n**. The vector from the origin to L_{ei} for link numbers k = 0, 1, and 2 is given as follows:

$$\boldsymbol{le_{2k}} = \boldsymbol{c} + \boldsymbol{R} \begin{pmatrix} R_s \cos\left(\frac{2\pi}{3} n - \frac{D_s}{2}\right) \\ R_s \sin\left(\frac{2\pi}{3} n - \frac{D_s}{2}\right) \\ 0 \end{pmatrix} \tag{3}$$

$$\boldsymbol{le}_{2k+1} = \boldsymbol{c} + \boldsymbol{R}\begin{pmatrix} R_e \cos(\frac{2\pi}{3}n + \frac{D_e}{2}) \\ R_e \sin(\frac{2\pi}{3}n + \frac{D_e}{2}) \\ 0 \end{pmatrix} \quad (4)$$

Given that the link length L_c is constant, the displacement by each axis by the prismatic actuator is given by

$$\mathbf{lb}_{nz} = \boldsymbol{le}_{nz} - \sqrt{l_c^2 - (\boldsymbol{le}_{nx} - \boldsymbol{lb}_{nx})^2 - (\boldsymbol{le}_{ny} - \boldsymbol{lb}_{ny})^2} \quad (5).$$

C. Simulator

A simulator (Figure 4) was developed for determining the design parameters of the parallel mechanism to facilitate intuitive designing. This simulator enables the design parameters to be easily checked, and the user can visually confirm if the predefined parameters can satisfy the workspace requirement by virtually dragging the tip of the end effector (i.e., instrument). Using this simulator, the parameters were defined as L_{eff} = 124 mm, L_c = 35.4 mm, f = 164.1 mm, R_e = 20 mm, D_e = 30°, R_b = 21 mm, D_b = 60°, θ_0 = 25°, and L_{max} = 50 mm.

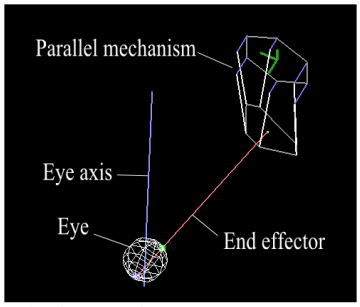

Fig.4 Parallel mechanism simulator

D. Development of robot

By using the parameters obtained using the simulator, the miniature parallel robot was developed as shown in Fig. 5. Plastic universal joints with a zero-backlash mechanism (MCM-9-4, Mighty Corporation Ltd.), linear actuators (20DAM10D2U-L, Danaher Corporation), and miniature linear guides were used to reduce the weight of the robot. The designed parallel mechanism has a theoretical positioning resolution of 12.7 μm.

As mentioned above, the parallel mechanism enables 3-DOF motion for positioning. Therefore, two actuators were implemented for manipulating the instrument. 360° rotation around the instrument axis was actuated by a belt drive using a stepping motor (SPG20-361, Nidec Copal Corporation). The tip of the micro forceps used in actual clinical cases was attached to the robot, and the gripper of the forceps was actuated using a linear actuator (20DAM10D2U-K, Danaher Corporation).

Fig. 5 shows the developed miniature parallel robot and Fig. 6, the emergency instrument retraction mechanism. The base of the instrument is retracted inside the robotic frame by 30 mm using coil springs when the locking mechanism is manually released by moving the two locking plates. A part connecting the robot and the forceps can be easily removed; this facilitates the interchange of the instrument without the risk of contamination. The robot itself does not need to be sterilized because it can be covered during the operation. The size of the developed robot is 85 mm × 100 mm × 240 mm and its weight is 770 g, which satisfies the design requirements.

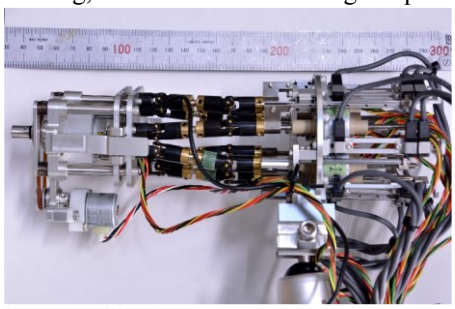

Fig. 5 Miniature parallel robot

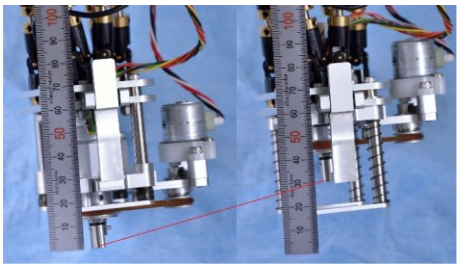

Fig. 6 Emergent instrument retraction

The developed robot was mounted on an endoscopic holder (Point Setter Endoscope Holder, Mitaka Kohki Co., Ltd., Japan). Control using a master manipulator for microsurgery [8] was implemented (Fig. 7).

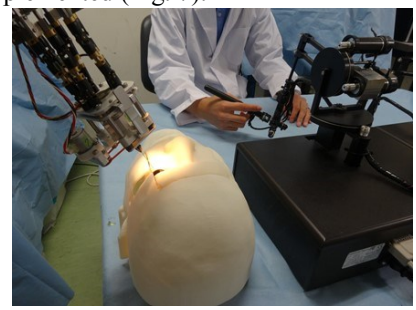

Fig.7 Master-slave robotic system for eye surgery

III. Experiments

The fundamental performance of the developed robot and its potential clinical applications were experimentally validated.

A. Fundamental performance

After confirming the motions along all axes and the usability of the system, motion errors at the RCM point were measured by tracing the edge of the workspace (i.e., a circle of 7 mm) with the tip of a micropipette mounted on the robot using the master manipulator with a motion scaling ratio of 1/50. The measured maximum error was 6.9 mm. The access to the defined workspace was confirmed, but the average error was larger than the acceptable error of 3 mm.

The positioning accuracy was measured by tracing a square of side 1 mm with the tip the micropipette using the master

manipulator (Fig. 8). The average positioning error was 40.0 μm. The error was caused by the manipulation error, hand tremor and backlash of the mechanisms. The error was smaller than that of the manual operation but larger than that of the previously developed robot [5] due to backlash. Both the mechanisms and control need to be further improved to increase the accuracy.

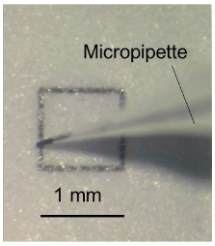

Fig. 8 Tracing experiment

B. *Peeling of ILM model*

In addition to the basic performance test, a membrane peeling test that simulated ILM peeling in vitreoretinal surgery was performed to demonstrate the validity of the system in a clinical setting. An artificial ILM model of 2.5-μm thickness that simulated the mechanical properties of the ILM membrane was used in the experiment as shown in Fig. 9, and the force applied by the robotic forceps on the ILM model was measured by placing a custom-made force sensor under the ILM model. Two engineering students were recruited for this experiment, and they performed the membrane peeling task with and without the robotic aid.

Fig. 10 shows the force applied in the vertical direction during the peeling of the ILM model. The average maximum force during peeling was 489 and 276 mN for the manual and the robotic task, respectively. The average task completion time was 146 and 105 s for the manual and the robotic task, respectively. Although it is difficult to draw conclusions based on only two subjects, the experimental results suggest that the robotic system can significantly decrease the force on the retina, making the surgery safer. The number of subjects needs to be further increased to discuss the differences between engineering students and medical doctors.

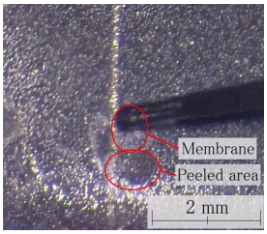

Fig. 9 Peeling of ILM model

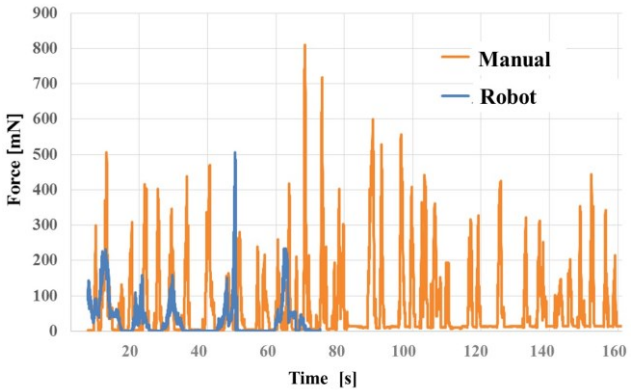

Fig. 10 Force applied on ILM model

IV. Conclusion

A 5-DOF miniature parallel robot with an emergency instrument retraction function has been developed for eye surgery. This robot is controlled by the master manipulator for microsurgery. Its size is 85 mm × 100 mm × 240 mm, and its weight is 770 g. Furthermore, its tracing accuracy was 40.0 μm. Experimental results of ILM model peeling suggested that this robot can effectively reduce the force applied on the retina. Further experiments will be conducted to validate its performance after improving the mechanisms and control.

Acknowledgments

The authors thank Prof. F. Arai and Mr. I. Kato of Nagoya University for their advice and for providing the ILM models.

References

[1] SPN. Singhy and CN. Riviere, "Physiological Tremor Amplitude during Retinal Microsurgery," IEEE 28th Annual Northeast Bioengineering Conference, pp. 171–172, 2002.

[2] A. Uneri, M. A. Balicki, J. Handa, P. Gehlbach, R. H. Taylor, and I. Iordachita, "New Steady-Hand Eye Robot with Micro-Force Sensing for Vitreoretinal Surgery," IEEE/RAS-EMBS International Conference on Biomedical Robotics and Biomechatronics (EMBC 2010), pp. 814–819, 2010.

[3] S. Yang, R. A. MacLachlan, and C. N. Riviere, "Design and Analysis of 6 DOF Handheld Micromanipulator," IEEE International Conference on Robotics and Automation (ICRA 2012), pp. 1946–4729, 2012.

[4] A. Gijbels, N. Wouters, P. Stalmans, H. Van Brussel, D. Reynaerts, and E. Vander Poorten, "Design and Realisation of a Novel Robotic Manipulator for Retinal Surgery," 2013 IEEE/RSJ International Conference on Intelligent Robots and Systems (IROS 2013), pp. 3598–3603, 2013.

[5] T. Nakano, N. Sugita, T. Ueta, Y. Tamaki, and M. Mitsuishi, "A Parallel Robot to Assist Vitreoretinal Surgery," International Journal of Computer Assisted Radiology and Surgery. 2009: 4 (6) 517–526.

[6] Y. Ida, N. Sugita, T. Ueta, Y. Tamaki, K. Tanimoto, and M. Mitsuishi, "Microsurgical Robotic System for Vitreoretinal Surgery," International Journal for Computer Assisted Radiology and Surgery. 2012; 7(1) 27–34.

[7] J. P. Merlet, Parallel Robots, Springer, 2006.

[8] Y. Kamei, K. Harada, S. Tanaka, Y. Kurose, Y. Baek, S. Sora, A. Morita, N. Sugita, M. Mitsuishi,"Master manipulator with high usability designed for microsurgical robotic system", International Journal of Computer Assisted Radiology and Surgery, 8, suppl.1, S127, 2013.